Vibrational Quenching of Optically Pumped Carbon Dimer Anions

Markus Nötzold,[1] Robert Wild,[1] Christine Lochmann,[1] Tanja Rahim,[1] Sruthi Purushu Melath,[1] Katrin Dulitz,[1] Barry Mant,[1] Jan Franz,[2] Francesco A. Gianturco,[1] and Roland Wester[1,*]

[1]*Institut für Ionenphysik und Angewandte Physik, Universität Innsbruck, Technikerstraße 25, 6020 Innsbruck, Austria*

[2]*Faculty of Applied Physics and Mathematics and Advanced Materials Center, Gdańsk University of Technology, 80-233 Gdańsk, Poland*

(Received 13 November 2022; revised 8 August 2023; accepted 25 September 2023; published 30 October 2023)

Careful control of quantum states is a gateway to research in many areas of science such as quantum information, quantum-controlled chemistry, and astrophysical processes. Precise optical control of molecular ions remains a challenge due to the scarcity of suitable level schemes, and direct laser cooling has not yet been achieved for either positive or negative molecular ions. Using a cryogenic wire trap, we show how the internal quantum states of C_2^- anions can be manipulated using optical pumping and inelastic quenching collisions with H_2 gas. We obtained optical pumping efficiencies of about 96% into the first vibrational level of C_2^- and determined the absolute inelastic rate coefficient from $v = 1$ to 0 to be $k_q = (3.2 \pm 0.2_{stat} \pm 1.3_{sys}) \times 10^{-13}$ cm^3/s at 20(3) K, over 3 orders of magnitude smaller than the capture limit. Reduced-dimensional quantum scattering calculations yield a small rate coefficient as well, but significantly larger than the experimental value. Using optical pumping and inelastic collisions, we also realized fluorescence imaging of negative molecular ions. Our work demonstrates high control of a cold ensemble of C_2^-, providing a solid foundation for future work on laser cooling of molecular ions.

DOI: 10.1103/PhysRevLett.131.183002

Cooling and controlling quantum states of molecular ions [1–3] is an enabling technology that has opened up a large field of research on precise studies of elastic and inelastic collision processes [4–6], controlled chemical reactions [7,8], as well as on novel precision spectroscopy and measurements of fundamental constants [9–11]. Over the last years, the research of negative ions gained interest due to their proposed application to sympathetically cool antiprotons [12], thus providing a new method of producing cold antihydrogen [13] in large abundance. However, the loosely bound excess electron in an anion makes it a more fragile system in which multiple electronic states are rarely encountered unless in the form of a dipole bound state [14–16] close to the detachment threshold. Only few atomic negative ions are known to possess valence excited electronic states. To prepare for negative ion laser cooling these anions have been explored in high-resolution spectroscopy [17–19]. An interesting alternative are small molecular anions, in particular the carbon dimer anion C_2^- [20]. Recently, we have determined the frequency of one out of two possible laser cooling transitions in this anion with suitable accuracy [21].

To achieve laser cooling of molecules, control of the vibrational level population using repumping lasers is imperative, as nondiagonal Franck-Condon factors lead to radiative decay into excited vibrational levels that must be returned into the optical cycle [22]. It is therefore interesting to explore vibrational state-changing collisions, because they may counteract optical pumping or even offer opportunities to reduce the number of repumping lasers, in particular for vibrational levels with small branching ratios where the impact of collisional heating of translational motion is small. The combination of collisional cooling of rotational states with sympathetic cooling of the translational degrees of freedom with laser-cooled ions has been demonstrated in a Coulomb crystal of Mg^+ and MgH^+ in a dilute gas of neutral helium [5]. Furthermore, in a buffer gas-cooled ion cloud quenching collisions allow one to close the cycling transition and apply fluorescence detection. For rotational state-changing inelastic collisions, absolute cross section data have become available using quantum scattering calculations [23–25] and state-resolved collision experiments in a cryogenic ion trap [6,26]. Vibrationally inelastic collisions are substantially more challenging to calculate, as the rigid rotor assumption is no longer applicable. Precise calculations have up to now only been carried out for diatomic ions colliding with atoms [27,28]. Experimentally, vibrational quenching collisions of mostly atmospherically relevant molecular ions have been studied at 300 K and above [29–32].

In this Letter we demonstrate optical pumping of the C_2^- anion into its first vibrational level $v = 1$ with high efficiency and measure the absolute rate coefficient for collisional quenching back into the ground vibrational level $v = 0$ in collisions with molecular hydrogen at a temperature of 18 K. H_2 is chosen, because calculations of

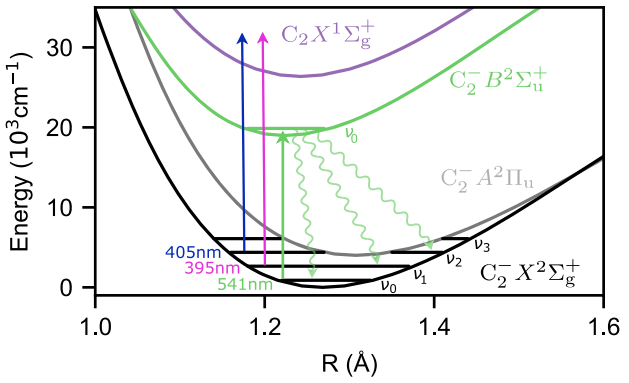

FIG. 1. Potential energy curves and lowest vibrational levels of C_2^-. A 541 nm beam is used to drive the $B^2\Sigma_u^+(v=0, J=1/2, 3/2) \leftarrow X^2\Sigma_g^+(v=0, J=1/2)$ transition. From the $B^2\Sigma_u^+$ state the anions spontaneously decay to different vibrational levels of the $X^2\Sigma_g^+$ state. A 395 nm beam neutralizes anions in $v=1$ and higher levels, while a 405 nm beam neutralizes anions in $v=2$ and higher.

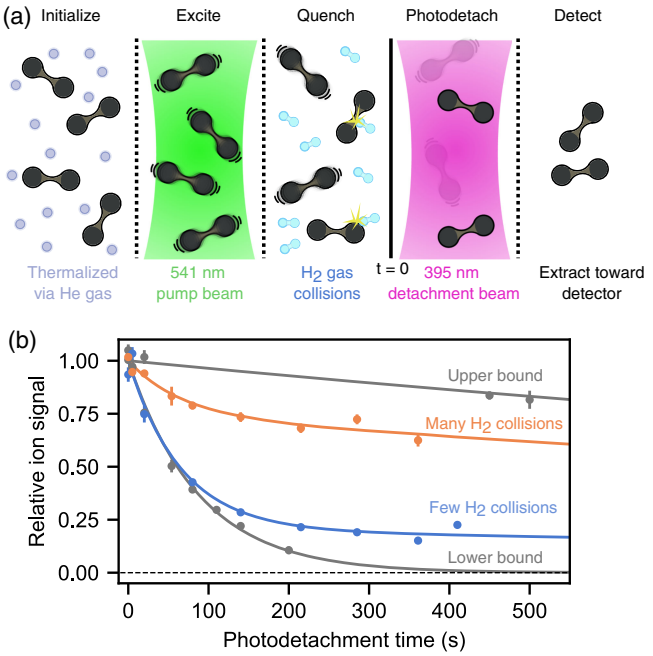

FIG. 2. (a) Steps for obtaining the vibrational excited state fraction of an ensemble of C_2^- anions after interaction with H_2 gas: thermalization with helium gas, optical pumping into $v=1$, addition of H_2 to quench a fraction of the anions into $v=0$, and finally photodetachment of anions in $v=1$ and higher with another light beam and detection of the remaining ions. (b) Ion signal for various exposure times to the 395 nm photodetachment beam. The blue and orange curve show the ion signal for about 1500 and 6500 collisions with the H_2 gas, respectively. The upper bound is measured by omitting the 541 nm pump laser and only measuring the loss from the trap due to the photodetachment beam and background losses. The lower bound is measured by continuously pumping the ensemble with the pump laser while the detachment beam is active. The solid lines are the fit functions described by Eq. (2).

quenching collisions with helium atoms show a currently unmeasurably small rate coefficient [27]. Photodetachment near threshold is used to probe the vibrational levels of C_2^-. We compare the measured quenching rate coefficient with quantum scattering calculations. Building on the rovibrational quenching, we then demonstrate direct fluorescence imaging of a cloud of trapped C_2^- ions, which shows a successful closure of the optical cycling transition via collisions.

In the experiment, a beam at 541 nm is used to pump the anions from the electronic ground state $X^2\Sigma_g^+$ into the second electronic excited state $B^2\Sigma_u^+$ (see Fig. 1). From there, the anions decay spontaneously to different vibrational levels of the electronic ground state. Using a 395 nm beam, anions in $v=1$ and higher lying levels can be selectively removed by photodetachment, $C_2^- + h\nu \longrightarrow C_2 + e^-$. Alternatively, a 405 nm beam can neutralize anions in $v \geq 2$.

The employed experimental setup consists of a radio-frequency multipole wire ion trap mounted on a cryostat, which is kept at a temperature of 18 K to avoid H_2 freezing to the walls of the ion trap. The design, which is a slightly modified version of the one presented in [33], combines the advantages of buffer gas cooling in a multipole trap [34] with enhanced optical access due to the use of thin wires. C_2^- anions are created from a plasma discharge source using acetylene seeded in argon and are selectively loaded into the trap via time of flight (see Supplemental Material for more information [35]).

Once the ions are trapped, the measurement procedure continues as illustrated in Fig. 2(a). In the first step, the anions' translational and rotational temperature are thermalized with a helium buffer gas at 18 K, thus creating a kinetic energy and rotational level distribution close to a thermal Maxwell-Boltzmann distribution. Afterward, the anions are optically excited via the $B^2\Sigma_u^+(v=0, J=1/2, 3/2) \leftarrow X^2\Sigma_g^+(v=0, J=1/2)$ transition, which is followed by radiative decay into the vibrational levels of the electronic ground state governed by angular momentum selection rules and Franck-Condon factors [20]. The helium buffer gas redistributes the rotational levels within a vibrational level with a calculated rate coefficient close to the Langevin rate [51], which yields a thermalization timescale of about a millisecond. The vibrational level distribution is not expected to be affected by the helium atoms, as the calculated cross section for vibrational deexcitation is 8 orders of magnitude smaller than for rotational state changing collisions [27]. Hence, the helium gas in combination with the pump beam enables us to excite anions into higher vibrational levels even if they are initially not in the lowest rotational state that is addressed by the pump laser.

The vibrational ground level of the electronic $A^2\Pi_u^+$ state is lower in energy than the $v=3$ state of the electronic

$X^2\Sigma_g^+$ state. Thus, electronic ground state ions in $v = 3$ and higher can decay into the $A^2\Pi_u^+$ state via dipole-allowed electronic transitions. From there, they can then further decay into $v = 0$, 1, 2 of the $X^2\Sigma_g^+$ state. Consequently, we only expect ions to be in $v = 1$ and $v = 2$ after the 15 s long optical pumping step. According to the Franck-Condon factors, one would expect about 80% of the ion ensemble to be in $v = 1$ and 20% in $v = 2$ [52,53]. When measuring the photodetachment loss signal of $C_2^-(v = 2)$ using the 405 nm laser, only a very small decay rate, corresponding to a population in $v = 2$ of about 1%, is measured. About 96(2)% of the ions are pumped into $v = 1$, with the remaining fraction being in $v = 0$. This is attributed to small amounts of residual H_2 in the experimental setup that interacts with the trapped ions, which quenches most of the $v = 2$ population and a small fraction of the anions in $v = 1$ during the 15 s optical pumping time in agreement with a rate equation model.

With the ensemble of C_2^- anions prepared predominantly in the $v = 1$ level, an H_2 gas pulse with a controllable density and duration is added to the trap. After a chosen interaction time with the H_2 gas, a 395 nm beam is shone into the trap, removing all anions that remain in $v = 1$ [see Fig. 2(a)]. As a final step, the anions that are in $v = 0$ are extracted from the trap and are destructively measured on a microchannel plate detector. By changing the density and duration of the H_2 gas pulse, the amount of anions quenched into the $v = 0$ state, and thus the number of anions detected, varies. This is illustrated in Fig. 2(b) where the ion signal is shown as a function of the detachment time for different densities of H_2 gas injected into the trap. The higher the gas density, the more ions are collisionally deexcited, and hence the higher is the detected ion signal at long photodetachment times.

To extract the fraction of quenched ions from the measured ion signal, a rate equation model is utilized. The equations that describe the change of the relative ion signal depend on the molecules in the first vibrational excited state N_1 and the vibrational ground state N_0 via

$$\dot{N}_1 = -N_1 k_1^{\mathrm{pd}} - N_1 k_{\mathrm{bg}}, \tag{1a}$$

$$\dot{N}_0 = -N_0 k_0^{\mathrm{pd}} + N_1 k_{\mathrm{bg}}. \tag{1b}$$

Here k_1^{pd} and k_0^{pd} are the 395 nm photodetachment rates of anions in $v = 0$ and 1, respectively, and k_{bg} is the quenching rate due to background gas. The background gas is the finite amount of gas always present in the system and mostly consists of H_2 as a large fraction of the other gas species freeze to the cryostat. Note that k_0^{pd} is not zero because of the spectral width of the 395 nm diode which also causes a small photodetachment rate for ions in $v = 0$. We find k_{bg} to be negligible in comparison to k_1^{pd} (see Supplemental Material [35]), thus the equations decouple yielding a simple solution for the total anion number

$$N_0(t) + N_1(t) = C_1\, \mathrm{e}^{-k_1^{\mathrm{pd}} t} + C_0\, \mathrm{e}^{-k_0^{\mathrm{pd}} t}, \tag{2}$$

where C_1 and C_0 are left as free parameters when used as a fitting function and define the amplitude of the ions in the $v = 1$ or $v = 0$ state. With the excited state fraction at time $t = 0$ defined as $C_{\mathrm{e}} = [C_1/(C_1 + C_0)]$ and after correction of the amplitudes via a background measurement (see Supplemental Material), we can calculate the quenching rate coefficient k_{q} due to a prior gas pulse of density n_0 and duration t_0 as

$$k_{\mathrm{q}} = \frac{-\ln(C_{\mathrm{e}})}{n_0 t_0}. \tag{3}$$

Using the Langevin rate coefficient the number of ion-neutral collisions that overcome the centrifugal barrier and reach short interatomic distances is determined for a given time and density of an H_2 gas pulse. The excited state fraction C_{e} is then plotted as a function of the number of H_2 collisions in Fig. 3(a). From the slope of an exponential fit to these data, which amounts to $0.19(1)_{\mathrm{stat}} \times 10^{-3}$ per collision, the quenching rate coefficient is obtained as $k_{\mathrm{q}} = (3.2 \pm 0.2_{\mathrm{stat}} \pm 1.3_{\mathrm{sys}}) \times 10^{-13}\ \mathrm{cm}^3/\mathrm{s}$ at 20(3) K. The error on the rate includes a 40% systematic error stemming from the pressure measurement of the gas pulse. The value and error of the ion temperature are extracted from molecular dynamics simulations and Doppler width measurements [21] suggesting an ion temperature slightly higher than the cryostat temperature of 18 K.

The measured rate is compared with theoretical calculations in Fig. 3(b). The theoretical curves are obtained by reduced-dimensional quantum scattering calculations carried out using the coupled channel method for scattering of an atom with a diatomic molecule as implemented in the ASPIN code [36] (see Supplemental Material [35]). The calculations predict an H_2 quenching rate coefficient that is about a factor of two higher than for argon and about 6 orders of magnitude larger than for helium [27]. Furthermore, the rate increases with decreasing collision temperature and the quenching rate $v_2 \longrightarrow v_1$ is significantly faster than $v_1 \longrightarrow v_0$ which is linked to the reduced energy gap in the former process. The measured rate coefficient for the $v_1 \longrightarrow v_0$ quenching process is about a factor of 13 smaller than the theoretical prediction, which is substantially outside of the estimated experimental uncertainty. Systematic tests of the *ab initio* calculations have shown that they are not expected to change significantly with a larger basis set or an explicitly correlated method of computation. Instead, it seems likely that the reason for the disagreement between theory and experiment is that the six internal degrees of freedom in the C_2^--H_2 system had to be reduced to three to perform the calculation. This is supported by earlier studies of the neutral CO-H_2 system, where only a full dimensional calculation [54] provided rate coefficients in good agreement with

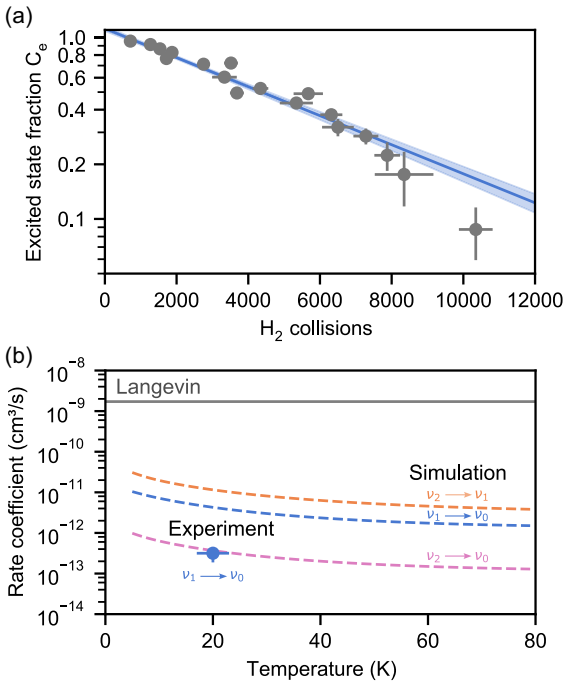

FIG. 3. (a) Fraction of C_2^- molecules in the first vibrational excited state as a function of collisions with H_2. The blue curve is an exponential fit to determine the quenching rate. The error bars are the 1-σ error, calculated using Gaussian error propagation. The shaded area shows the 1-σ confidence band of the fit parameters. (b) Measured quenching rate coefficient obtained via fit of an exponential function from (a).

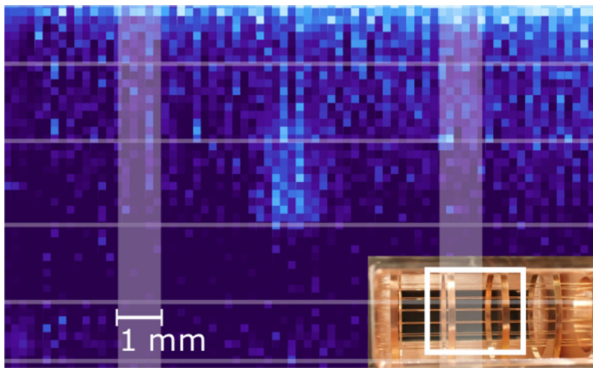

FIG. 4. Fluorescence image of C_2^-. The inset shows a photograph of the multipole wire trap with wires and ring electrodes, which was operated in octupole mode by pairing neighboring wires. The locations of the electrodes have been overlaid with the fluorescence image for scale. The ion cloud is visible in the center of the trap via spontaneous emission at 598 nm, whereas the scattered light at the top of the image results from incompletely filtered light from the pump laser at 541 nm.

experiments [55]. Consequently, a full six-dimensional treatment also seems necessary here and calculations by our group are under way.

The experimentally obtained quenching rate is about 4 orders of magnitude smaller than the Langevin rate of $k_L = 1.7 \times 10^{-9}$ $(\mathrm{cm}^3/\mathrm{s})$ as well as the inelastic quenching rate coefficient for rotational levels [51]. The rate is also 10 times smaller than room-temperature measurements of O_2^+ cations [30], which can be explained by the weaker short-range interaction of negative ions compared to positive ions. According to calculations, helium and neon atoms, which are less polarizable than H_2, feature even a vastly smaller rate coefficients [27]. This makes H_2 the most feasible neutral species to collisionally deexcite vibrational levels of C_2^-.

Collisional repumping can be used as a method to close a cycling transition of C_2^- without the need for a large set of repumping laser beams. To illustrate this we imaged the spontaneous emission of C_2^- onto an EMCCD camera, as seen in Fig. 4. We used only the primary 541 nm pump beam and inelastic collisions with H_2 to transfer the ions back to the rovibrational ground state. A bandpass filter for photons near 598 nm, corresponding to the $B^2\Sigma_u^+(v = 0) \longrightarrow X^2\Sigma_g^+(v = 1)$ transition, was included, which suppressed scattered light from the 541 nm beam. The image corresponds to approximately 2000 ions with an estimated total photon scattering rate per ion of about 40 s^{-1} into the full solid angle. Such direct fluorescence measurements are not routinely available for molecular ions and will prove useful for further studies of state-resolved collisions and cooling techniques.

The presented scheme can also be applied to other molecular anions, including polyatomic species, when possessing multiple electronic states. In the future laser-cooled negative ions, combined with ultracold positive ions, may open up research on frozen quasineutral plasmas. They will also allow cooling of antiprotons for a more efficient production of antihydrogen atoms and or even antihydrogen molecules. Because of the absence of any electric dipole moment, the internal quantum states of carbon chain anions are very resilient to electric fields. This offers interesting perspectives for a unique new trapped ion qubit realization.

This work has been supported in part by the Austrian Science Fund (FWF), Projects No. P29558-N36 and No. I3159-N36. We acknowledge that the results of this research have been achieved using the DECI resource BEM based in Poland at WCSS with support from the PRACE aisbl. The computational results have in parts also been obtained using the LEO HPC infrastructure of the University of Innsbruck.

*roland.wester@uibk.ac.at

[1] T. Schneider, B. Roth, H. Duncker, I. Ernsting, and S. Schiller, Nat. Phys. **6**, 275 (2010).
[2] P. F. Staanum, K. Højbjerre, P. S. Skyt, A. K. Hansen, and M. Drewsen, Nat. Phys. **6**, 271 (2010).

[3] P. R. Stollenwerk, M. G. Kokish, A. G. S. De Oliveira-Filho, F. R. Ornellas, and B. C. Odom, Atoms **6**, 53 (2018).
[4] W. G. Rellergert, S. T. Sullivan, Steven, J. Schowalter, S. Kotochigova, K. Chen, and E. R. Hudson, Nature (London) **495**, 490 (2013).
[5] A. K. Hansen, O. O. Versolato, L.Klosowski, S. B. Kristensen, A. Gingell, M. Schwarz, A. Windberger, J. Ullrich, J. R. C. Lopez-Urrutia, and M. Drewsen, Nature (London) **508**, 76 (2014).
[6] D. Hauser, S. Lee, F. Carelli, S. Spieler, O. Lakhmanskaya, E. S. Endres, S. S. Kumar, F. Gianturco, and R. Wester, Nat. Phys. **11**, 467 (2015).
[7] P. Puri, M. Mills, I. Simbotin, J. A. Montgomery, R. Côté, C. Schneider, A. G. Suits, and E. R. Hudson, Nat. Chem. **11**, 615 (2019).
[8] A. D. Dörfler, P. Eberle, D. Koner, M. Tomza, M. Meuwly, and S. Willitsch, Nat. Commun. **10**, 5429 (2019).
[9] M. Germann, X. Tong, and S. Willitsch, Nat. Phys. **10**, 820 (2014).
[10] F. Wolf, Y. Wan, J. C. Heip, F. Gebert, C. Shi, and P. O. Schmidt, Nature (London) **530**, 457 (2016).
[11] S. Patra, M. Germann, J.-P. Karr, M. Haidar, L. Hilico, V. Korobov, I, F. M. J. Cozijn, K. S. E. Eikema, W. Ubachs, and J. C. J. Koelemeij, Science **369**, 1238 (2020).
[12] G. Cerchiari, A. Kellerbauer, M. S. Safronova, U. I. Safronova, and P. Yzombard, Phys. Rev. Lett. **120**, 133205 (2018).
[13] C. Baker, W. Bertsche, A. Capra, C. Carruth, C. Cesar, M. Charlton, A. Christensen, R. Collister, A. C. Mathad, S. Eriksson *et al.*, Nature (London) **592**, 35 (2021).
[14] K. R. Lykke, R. D. Mead, and W. C. Lineberger, Phys. Rev. Lett. **52**, 2221 (1984).
[15] D.-F. Yuan, Y. Liu, C.-H. Qian, Y.-R. Zhang, B. M. Rubenstein, and L.-S. Wang, Phys. Rev. Lett. **125**, 073003 (2020).
[16] M. Simpson, M. Nötzold, T. Michaelsen, R. Wild, F. A. Gianturco, and R. Wester, Phys. Rev. Lett. **127**, 043001 (2021).
[17] U. Warring, M. Amoretti, C. Canali, A. Fischer, R. Heyne, J. O. Meier, C. Morhard, and A. Kellerbauer, Phys. Rev. Lett. **102**, 043001 (2009).
[18] E. Jordan, G. Cerchiari, S. Fritzsche, and A. Kellerbauer, Phys. Rev. Lett. **115**, 113001 (2015).
[19] R. Tang, R. Si, Z. Fei, X. Fu, Y. Lu, T. Brage, H. Liu, C. Chen, and C. Ning, Phys. Rev. Lett. **123**, 203002 (2019).
[20] P. Yzombard, M. Hamamda, S. Gerber, M. Doser, and D. Comparat, Phys. Rev. Lett. **114**, 213001 (2015).
[21] M. Nötzold, R. Wild, C. Lochmann, and R. Wester, Phys. Rev. A **106**, 023111 (2022).
[22] M. R. Tarbutt, Contemp. Phys. **59**, 356 (2018).
[23] K. M. Walker, F. Lique, F. Dumouchel, and R. Dawes, Mon. Not. R. Astron. Soc. **466**, 831 (2016).
[24] M. Hernandez-Vera, F. A. Gianturco, R. Wester, H. da Silva Jr, O. Dulieu, and S. Schiller, J. Chem. Phys. **146**, 124310 (2017).
[25] B. Mant, F. Gianturco, L. Gonzalez-Sanchez, E. Yurtsever, and R. Wester, J. Phys. B **53**, 025201 (2020).
[26] F. A. Gianturco, O. Y. Lakhmanskaya, M. Hernández Vera, E. Yurtsever, and R. Wester, Faraday Discuss. **212**, 117 (2018).
[27] B. P. Mant, F. A. Gianturco, R. Wester, E. Yurtsever, and L. González-Sánchez, Phys. Rev. A **102**, 062810 (2020).
[28] B. Mant, E. Yurtsever, L. González-Sánchez, R. Wester, and F. A. Gianturco, J. Chem. Phys. **154**, 084305 (2021).
[29] B. A. Huber, P. C. Cosby, J. R. Peterson, and J. T. Moseley, J. Chem. Phys. **66**, 4520 (1977).
[30] E. E. Ferguson, J. Phys. Chem. **90**, 731 (1986).
[31] S. Kato, V. M. Bierbaum, and S. R. Leone, Int. J. Mass Spectrom. Ion Process. **149**, 469 (1995).
[32] W. Singer, A. Hansel, A. Wisthaler, W. Lindinger, and E. Ferguson, Int. J. Mass Spectrom. **223**, 757 (2003).
[33] K. Geistlinger, M. Fischer, S. Spieler, L. Remmers, F. Duensing, F. Dahlmann, E. Endres, and R. Wester, Rev. Sci. Instrum. **92**, 023204 (2021).
[34] R. Wester, J. Phys. B **42**, 154001 (2009).
[35] See Supplemental Material at http://link.aps.org/supplemental/10.1103/PhysRevLett.131.183002 for a detailed description, which includes Refs. [33,36–50].
[36] D. Lopez-Duran, E. Bodo, and F. A. Gianturco, Comput. Phys. Commun. **179**, 821 (2008).
[37] M. Cafiero and L. Adamowicz, Phys. Rev. Lett. **89**, 073001 (2002).
[38] T. Takaishi and Y. Sensui, Trans. Faraday Soc. **59**, 2503 (1963).
[39] S. Furuyama, Bull. Chem. Soc. Jpn. **50**, 2797 (1977).
[40] I. Yasumoto, J. Phys. Chem. **84**, 589 (1980).
[41] K. Poulter, M.-J. Rodgers, P. Nash, T. Thompson, and M. Perkin, Vacuum **33**, 311 (1983).
[42] H.-J. Werner, P. J. Knowles, G. Knizia, F. R. Manby, M. Schütz *et al.* (2019), see https://www. molpro.net.
[43] R. J. Le Roy, J. Quant. Spectrosc. Radiat. Transfer **186**, 167 (2017).
[44] W. Shi, C. Li, H. Meng, J. Wei, L. Deng, and C. Yang, Comput. Theor. Chem. **1079**, 57 (2016).
[45] R. D. Mead, U. Hefter, P. A. Schulz, and W. C. Lineberger, J. Chem. Phys. **82**, 1723 (1985).
[46] F. Lique, R. Toboła, J. Kłos, N. Feautrier, A. Spielfiedel, L. F. M. Vincent, Chałasiński, and M. H. Alexander, Astron. Astrophys. **478**, 567 (2008).
[47] B. Mant, J. Franz, R. Wester, and F. A. Gianturco, Mol. Phys. **119**, e1938267 (2021).
[48] B. Yang, P. Zhang, X. Wang, P. C. Stancil, J. M. Bowman, N. Balakrishnan, and R. C. Forrey, Nat. Commun. **6**, 6629 (2015).
[49] B. Yang, P. Zhang, C. Qu, P. C. Stancil, J. M. Bowman, N. Balakrishnan, and R. C. Forrey, Chem. Phys. **532**, 110695 (2020).
[50] H.-J. Werner, B. Follmeg, and M. Alexander, J. Chem. Phys. **89**, 3139 (1988).
[51] B. P. Mant, F. A. Gianturco, R. Wester, L. Gonzalez, and E. Yurtsever, Int. J. Mass Spectrom. **457**, 116426 (2020).
[52] Y. Shan-Shan, Y. Xiao-Hua, L. Ben-Xia, K. Kakule, W. Sheng-Hai, G. Ying-Chun, L. Yu-Yan, and C. Yang-Qin, Chin. Phys. **12**, 745 (2003).
[53] W. Shi, C. Li, H. Meng, J. Wei, L. Deng, and C. Yang, Comput. Theor. Chem. **1079**, 57 (2016).
[54] B. Yang, P. Zhang, X. Wang, P. C. Stancil, J. M. Bowman, N. Balakrishnan, and R. C. Forrey, Nat. Commun. **6**, 6629 (2015).
[55] J. P. Reid, C. J. S. M. Simpson, and H. M. Quiney, J. Chem. Phys. **106**, 4931 (1997).